Dynamics of a Complete Wetting Liquid Under Evaporation

Chi-Tuong Pham, François Lequeux, Laurent Limat

Dynamics of a complete wetting droplet under evaporation

Chi-Tuong Pham[1], François Lequeux[2] and Laurent Limat[3]

[1] *Laboratoire LIMSI, Université Paris-Sud, Orsay, France*
[2] *Laboratoire PPMD, ESPCI & Université P. et M. Curie, Paris, France*
[3] *Laboratoire MSC, Université Paris Diderot, Paris, France*

Abstract: We describe a simple model of a contact line under purely diffusive evaporation and complete wetting condition taking into account the divergent nature of evaporative flux near the contact line as proposed by Deegan *et al.* [1] by using electrostatic analogy. We show the existence of a precursor film at the edge of the liquid and generalize Tanner's law accounting for evaporative effects. We apply this model to the problem of evaporation of a liquid droplet and partly recover the dynamics of spreading and retraction found in experiments [2].

Keywords: moving contact line, complete wetting

1 Introduction

Wetting phenomena have been extensively studied theoretically and experimentally (see Refs. [3–6] for reviews and discussions) and much attention has been drawn recently to the case of the dynamics of liquid droplet under evaporation. This problem is motivated by applications (for instance coating [7,8], deposition near contact line [9], heat exchangers [10, 11]) and by fundamental issues [12]. The local description of a moving contact line is a complicated problem for it involves a singularity of the viscous stresses due to no-slip boundary condition of the liquid on the substrate. The second phenomenon involved in the problem of evaporating contact line is the way the liquid evaporates. Two regimes shall be distinguished: on the first hand, evaporation of the liquid into its own vapor [11,13,14]; on the second hand, purely diffusive evaporation of the liquid in an inert surrounding gas [2, 15–17].

In this paper, we restrict ourself to the isothermal problem of a liquid evaporating into inert gas like air. Evaporation is then driven by diffusion. We describe in details a model of contact line under evaporation and total wetting conditions [15] taking into account van der Waals interactions and the divergent nature of evaporation near the border of the liquid as evidenced by Deegan et al. [1, 9] (section 2). We then apply this result to study the dynamics of an evaporating droplet in complete wetting situation (section 3) and compare the results with typical scaling laws of the dynamics of retraction of small droplets found in experiments [2, 18].

2 Low constant speed model

In this section, we study the shape of the free surface of an evaporating liquid corner moving at a *constant* velocity V along a totally wetting solid surface, both under the effect of a fluid motion $U(x, z)$ linked to pressure gradient, and of an evaporation flux $J(x)$. The edge of the liquid is set at $x = 0$ (see Fig.

1(Left) for notations). We suppose we have translation invariance along the transverse direction.

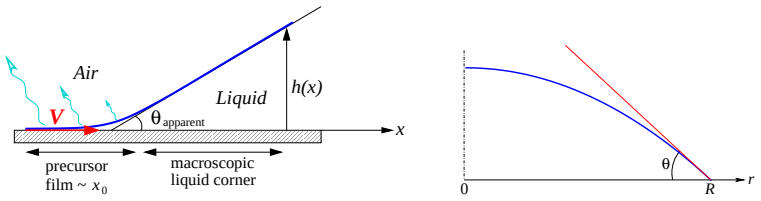

Figure 1: (Left) Notations for the model studied in Section 2 of a liquid moving at constant speed V on a totally wetting substrate and undergoing evaporation. (Right) Notations used in Section 3: R is the droplet radius and θ the apparent contact angle of the spherical cap.

Standard lubrication theory in the limit of low Reynolds numbers and small interface slope leads to a mean local velocity of the liquid given by: $\langle U\rangle = \frac{1}{h}\int_0^h U(x,z)\,\mathrm{d}z = -\frac{h^2}{3\eta}\frac{\partial P}{\partial x}$ where $h(x)$ is the liquid thickness, η the liquid viscosity, and the pressure term is

$$P = P_a + P_\mathrm{c} + P_\mathrm{d} \tag{1}$$

with P_a, the ambient pressure, P_c the capillary pressure and P_d, the disjoining pressure (we assume van der Waals interactions) playing a role at the edge of the liquid. Both latter pressures read respectively $P_\mathrm{c} = -\gamma h_{xx}$ and $P_\mathrm{d} = +\frac{\mathcal{A}}{6\pi h^3}$; γ is the surface tension and $\mathcal{A} < 0$ the Hamaker constant. In this problem, gravity will be neglected. For a liquid moving at constant velocity V, mass conservation imposes that the local thickness $h(x - Vt)$ satisfies

$$\partial_t h + \partial_x(h\langle U\rangle) + J(x) = 0, \tag{2}$$

which leads to:

$$\frac{\partial}{\partial x}\left[h\left(\langle U\rangle - V\right)\right] + J(x) = 0 \tag{3}$$

to be combined with the previous expression of $\langle U\rangle$.

One now needs an approximation of the local evaporation rate distribution $J(x)$. For a sessile axisymmetric drop, Deegan [9] assumed an analogy between vapor diffusion in air and an electrostatic problem, the vapor concentration near the liquid surface being supposed to saturate at the mass concentration in air c^sat. In analogy with this work, we assume that very near the edge of the liquid $J(x)$ diverges as $J(x) = J_0 x^{-(\pi/2-\theta)/(\pi-\theta)}$ where x is the distance to the edge. This yields for very small values of angle θ:

$$J(x) \approx J_0/\sqrt{x} \tag{4}$$

in which J_0 is given by

$$J_0 = \frac{D_g}{\sqrt{\lambda}}\frac{c^\mathrm{sat} - c^\infty}{\rho} \tag{5}$$

where D_g is the diffusion constant of evaporated liquid in air, and ρ its mass density. The length scale λ can be either the thickness of a diffusive boundary layer, or the typical curvature of the contact line. For instance, for the sessile

drops of in-plane radius R with low contact angle considered in Ref. [9] one has exactly $\lambda = 2R$. For volatile alkanes or silicon oil drops of millimetric size evaporating in ambient air one typically has $J_0 \approx 10^{-9}\ \mathrm{m}^{\frac{3}{2}} \cdot \mathrm{s}^{-1}$. Note that we are here treating the limit of a liquid evaporating in the presence of air. It is also important to note that the activity of a thin film of liquid is approximately that of the bulk up to the last molecular layer of liquid. Thus the divergence of the evaporative flux holds at the border of the precursor film. In our purely diffusive model, Marangoni and thermal gradients will be neglected.

After integrating once Eq. (3) with respect to x, one gets: $(< U > -V)h = -2J_0\sqrt{x}$ that can be written as:

$$V = \frac{2J_0}{h}\sqrt{x} + \frac{\gamma}{3\eta}h^2 h_{xxx} + \frac{\mathcal{A}}{6\pi\eta}\frac{h_x}{h^2} \tag{6}$$

The local thickness of liquid $h(x)$, is supposed to vanish or at least reach microscopic values at the tip of the liquid placed by hypothesis at the location $x = 0$.

The physical meaning of this equation is that the displacement of a liquid at velocity V involves migration under capillary and disjunction pressure gradient together with evaporation itself. This adds new terms to the ordinary differential equation governing $h(x)$, considered years ago by Voinov [19], that reads in this specific case:

$$h_{xxx} = \frac{3\mathrm{Ca}}{h^2} - \frac{6\eta J_0}{\gamma}\frac{\sqrt{x}}{h^3} - \frac{\mathcal{A}}{2\pi\gamma}\frac{h_x}{h^4} \tag{7}$$

where $\mathrm{Ca} = \eta V/\gamma$ is the capillary number built upon the velocity V ($\mathrm{Ca} > 0$ in the receding case and $\mathrm{Ca} < 0$ in the advancing case).

In the framework of this model, it is convenient to set a typical horizontal length scale x_0 and a typical height h_0 that respectively read

$$x_0 = \left(\frac{|\mathcal{A}|}{12\pi J_0\eta}\right)^{\frac{2}{3}}, \qquad h_0 = x_0^{\frac{1}{2}} \times \left(\frac{|\mathcal{A}|}{2\pi\gamma}\right)^{\frac{1}{4}} = \frac{|\mathcal{A}|^{\frac{7}{12}}}{(2\pi)^{\frac{7}{12}}(6\eta J_0)^{\frac{1}{3}}\gamma^{\frac{1}{4}}} \tag{8}$$

Setting $J_0 = 10^{-9}\,\mathrm{m}^{3/2}\cdot\mathrm{s}^{-1}$, $\mathcal{A} = 10^{-19}\,\mathrm{kg}\cdot\mathrm{m}^2\cdot\mathrm{s}^{-2}, \eta = 10^{-3}\,\mathrm{kg}\cdot\mathrm{m}^{-1}\cdot\mathrm{s}^{-1}$ yields typical lengths $x_0 \simeq 2\,\mu\mathrm{m}$ and $h_0 \simeq 30\,\mathrm{nm}$. These values have the same order of magnitude as those found experimentally by Kavehpour et al. [20] in the advancing regime *without* evaporation for $\mathrm{Ca} = 3 \times 10^{-4}$. The horizontal length x_0 corresponds in our model to the typical length of the precursor film at zero velocity.

Eq. (7) is third order in derivatives and the uniqueness of its solutions requires the specification of three boundary conditions at the border of the domain $\varepsilon \le x \le L_{\max}$. At large scale $L_{\max}$, we impose zero curvature ($h_{xx}(L_{\max}) = 0$). Two other boundary conditions are needed.

A solution vanishing at $x = 0$ that connects to a macroscopic liquid corner $h_{\mathrm{mac}}(x) = \theta_{\mathrm{mac}} \cdot x$ can be found at leading order in the neighborhood of zero as

$$h(x) = \alpha\sqrt{x} \quad \text{with} \quad \alpha^4 = \frac{2}{3\pi}\frac{|\mathcal{A}|}{\gamma} \tag{9}$$

This expression yields a crossover length

$$\ell_{\mathrm{cross}} \sim \frac{1}{\theta_{\mathrm{mac}}^2}\left(\frac{2}{3\pi}\frac{|\mathcal{A}|}{\gamma}\right)^{\frac{1}{2}}. \tag{10}$$

This class of solution has been found as well by Poulard *et al.* [2].

We can search for a second class of solutions that start flat ($h'(0) = 0$) at the origin at the given height $h(0) = h_0$. We can then obtain analytically, the expression of a precursor film the expression of which can be written as

$$H(X) = 1 + \nu_1 X^2 + cX^3 - \frac{8}{105} X^{\frac{7}{2}} + \frac{1}{12}\nu_1 X^4 + o(X^4) \tag{11}$$

with constants c depending on the capillary number and ν_1 insuring zero curvature at large scale. This precursor film connects to a large scale liquid corner profile, the expression of which is

$$\Theta^3(X) = \Theta_{\rm m}^3 - 9{\rm Ca}\left(\frac{x_0}{h_0}\right)^3 \ln\frac{X}{\lambda} + \frac{4}{\Theta_{\rm m}}\left(\frac{1}{\lambda^{\frac{1}{2}}} - \frac{1}{X^{\frac{1}{2}}}\right) + \beta(X - \lambda) \tag{12}$$

where $X = x/x_0, H = h(x)/h_0, \Theta(X) = H'(X)$ with $\Theta_{\rm m} \simeq 1$. Constant $\lambda \simeq 3.4$ is the matching coordinate between precursor and liquid corner. Constant β ensures the adequate boundary condition $H_{xx}(L_{\rm max}) = \Theta_X(L_{\rm max}) = 0$ (for calculations details, see Refs. [7,15]). Both analytical solutions (9) and (12) can be confirmed numerically using shooting methods. They are plotted in Fig. 2. The agreement is very good [15].

From Eq. (12), one can deduce the following expression for the apparent contact angle $\theta_{\rm app}$

$$\theta_{\rm app}^3 = \theta_{\rm m}^3 - 9{\rm Ca}\left(\log\frac{\mathcal{L}_{\rm macro}}{\ell_{\rm micro}} + 1\right) + \frac{24 J_0 \eta}{\gamma\theta_{\rm m}}\frac{1}{\sqrt{\ell_{\rm micro}}} \tag{13}$$

or in a more simplified way

$$\theta_{\rm app}^3 = \left(1 + \frac{4}{\sqrt{3.4}}\right)\theta_{\rm m}^3 - 9{\rm Ca}\left(\log\frac{\mathcal{L}_{\rm macro}}{\ell_{\rm micro}} + 1\right) \tag{14}$$

where $\ell_{\rm micro} \simeq 3.4 x_0$ is a microscopic length corresponding to the length of the precursor film, $\mathcal{L}_{\rm macro}$ a macroscopic length and

$$\theta_{\rm m}^3 = \left(\frac{h_0}{x_0}\right)^3 = \left(\frac{2\pi}{\gamma^3|\mathcal{A}|}\right)^{\frac{1}{4}} 6\eta J_0 \tag{15}$$

corresponding to the apparent contact angle at zero velocity [21]. This law generalizes Tanner's law in the presence of evaporation.

In a study of an evaporating meniscus in complete wetting situation where the coupling between the liquid and the gas is explicitly accounted instead of considering Deegan's electrostatic analogy as we do in this paper, Doumenc *et al.* derived a similar scaling for the apparent contact angle at zero velocity [17]. In this study, the authors splitted the liquid domain into different parts depending on the magnitude of the different physical effects involved in the problem (evaporation, capillary forces together with van der Waals forces). If we compare our model to theirs, our precursor film corresponds to the region they identify as the precursor film. The zero coordinate that we set as being the edge of the liquid corresponds to the beginning of their adsorbed film region. Note that the thickness we choose is one order of magnitude larger than theirs.

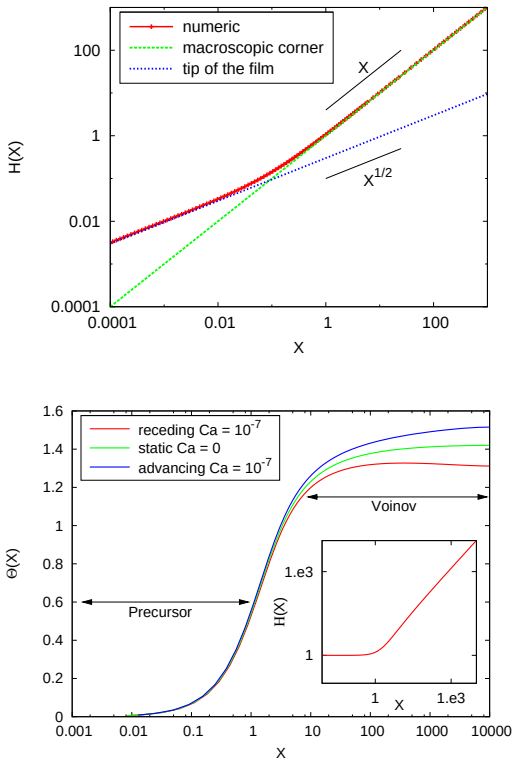

Figure 2: Numerical solutions of Eq. (7) in non dimensional units. (Top) Assuming vanishing height at origin: plot of $H(X)$ ($\mathrm{Ca} = +10^{-7}$). Two distinct scalings are observed: linear in the macroscopic domain and parabolic in the microscopic one (see straight lines). (Bottom) Assuming vanishing curvature at large distance (here $X_{\max} = 10^4$) and flat film at the edge of liquid: plot of angle Θ versus X (non dimensional unit). Inset: Corresponding $H(X)$ profile (receding case, same parameter): a macroscopic wedge is connected to a flat precursor film.

3 Evaporating sessile droplet

In this section, we will generalize our previous model and apply it to the study of an evaporating sessile droplet in total wetting condition. As already stated, the expression of the evaporative flux of a spherical cap of liquid of radius R, in the limit of small contact angle θ (see Fig. 1(Right)), reads $J(r) = j_0/\sqrt{R^2 - r^2}$ with the following correspondence with previous section: $x = R - r$, $J_0 = j_0/\sqrt{2R}$ and $\mathrm{Ca} = -\eta\dot{R}/\gamma$. Substituting directly these expressions into Eqs. (14) and (15) yields the following wetting law without any adjustable parameters (but a logarithmic contribution)

$$\theta^3 = \frac{A}{\sqrt{R}} + B\dot{R} \tag{16}$$

with

$$A = 6\,(\frac{\pi}{2})^{\frac{1}{4}} \left(1 + \frac{4}{\sqrt{3.4}}\right) \frac{\eta j_0}{\gamma^{\frac{3}{4}} |\mathcal{A}|^{\frac{1}{4}}} \qquad \text{and} \qquad B = 9\frac{\eta}{\gamma}\left(\log \frac{\mathcal{L}_{\text{macro}}}{\ell_{\text{micro}}} + 1\right). \tag{17}$$

This is the same kind of expression as that found by Poulard et al. using other arguments [2], hence we recover the same scaling for apparent angle at zero velocity (that is at maximum radius) $\theta_{\max} \sim R_{\max}^{-1/6}$ while experimental power law is $\theta_{\max} \sim R_{\max}^{-0.45}$.

A small sessile droplet can be considered as a spherical cap. At small contact angle θ, its volume V reads $V = \frac{\pi}{4} R^3 \theta$. Under diffusive evaporation, mass conservation reads $\frac{\mathrm{d}V}{\mathrm{d}t} = -\int_0^{2\pi} \int_0^R J(r) r \,\mathrm{d}r \,\mathrm{d}\varphi = -2\pi j_0 R$. Combining these two results yields the following relation

$$3R\theta\dot{R} + R^2\dot{\theta} = -8j_0. \tag{18}$$

With Eqs. (16) and (18) we then obtain a closed set of ordinary differential equations of variables R and θ that entirely governs the dynamics of evaporation of a droplet. We will now study this set of equations numerically.

Given the initial conditions $R_{\mathrm{i}} = R_{|t=0}$ and $\theta_{\mathrm{i}} = \theta_{|t=0}$, we can see using Eq. (16) that, whether $(\theta_{\mathrm{i}})^3\sqrt{R_{\mathrm{i}}}$ is larger or smaller than constant A, the droplet starts spreading then retracts, or directly starts with retraction. Experiments show that, if t_{f} is the time at which the droplet vanishes, the radius of a droplet of completely wetting alkane on mica follows the scaling $R(t) \sim (t_{\mathrm{f}} - t)^{\alpha}$ with exponent α close to $1/2$ [2,18]. During the retraction sequence, the contact angle θ has little variations up to late times before total evaporation [2]. Suppose that $R(t)$ scales like $(t_{\mathrm{f}} - t)^{\beta}$, Eq. (16) implies that $\beta = 2/3$ if θ is to remain bounded, which is not the case as we will see in the following.

We have performed numerical simulations of Eqs. (16) and (18) using same physical quantities as in experiments. Results are shown in Fig. 3. The dynamics of spreading followed by the retraction sequence of the droplet is recovered with correct orders of magnitude compared with experiments. As in the experiments [2], we recover the steep decrease of the contact angle during the spreading and the beginning of the retraction. Radius vanishes at a given final time t_{f}. In contrast, contact angle θ vanishes at time $t'_{\mathrm{f}} < t_{\mathrm{f}}$ (the spherical cap then becomes flat) and eventually becomes negative which is physically incorrect. This vanishing angle singularity is intrinsic to our wetting law model but experiments by Cazabat at al. also display sharp decrease of the contact angle at late times.

If one looks carefully at the decay of the radius $R(\tau)$ with time $\tau = t_{\mathrm{f}} - t$ (see Fig. 3 (Top)), one can see that the radius follows two regimes with distinct exponents. At the beginning of the retraction, $R(\tau) \sim \tau^{\alpha}$ with $\alpha \simeq 0.33$, then, once the values of θ becomes negative, we have $R(\tau) \sim \tau^{\beta}$ with $\beta \simeq 0.11$. These scalings are in disagreement with the experiments where exponents are close to $1/2$. Nevertheless, by choosing a shifted reference final time T_{f} (see inset of Fig. 3 (Bottom)), one can recover an exponent $\alpha' \simeq 0.45$ in agreement with experiments, as did Poulard et al. in their numerical simulations as well [2].

Note that our wetting law (16) contains a logarithmic term depending on a macroscopic scale $\mathcal{L}_{\text{macro}}$, at which contact angle is defined. Replacing the latter length scale by a fraction of radius R modifies the wetting law and shall

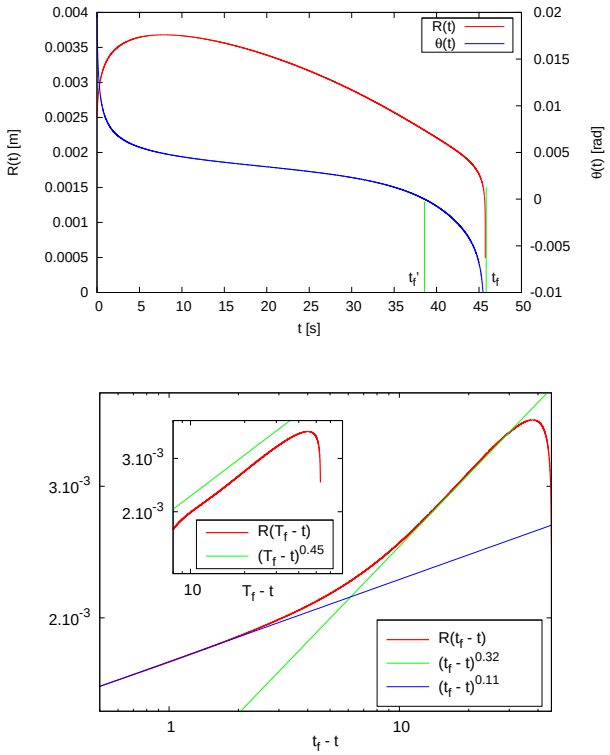

Figure 3: (Top) Plot versus time $t_\mathrm{f} - t$ of the radius R of an evaporating totally wetting droplet together with the angle θ. Time t_f corresponds to the time of vanishing radius whereas time t'_f if the time at which angle θ gets to zero. (Bottom) Plot of the dynamics of radius R in log-log scale. Depending on the choice of reference final time T_f, one obtains a different scaling and recovers that found in experiments.

delay the singularity (the smaller $\mathcal{L}_\mathrm{macro} \sim R$, the smaller constant B). We performed numerical simulations of the dynamics using this modified wetting law and found no major changes in the dynamics: the final time of singularity is slightly shifted but the scaling exponents remain the same (data not shown).

The wetting law described by Eq. 14 only catches the early dynamics of spreading and retraction of the droplet. Indeed this analytical model was derived in the hypothesis of translational invariance along transverse direction, constant speed limit and zero curvature at large scale which is not realistic for a spherical cap. Moreover, small capillary numbers were assumed whereas speed of retraction diverges at late times. In this context, the apparent contact angle in our model cannot remain finite. Yet simple, our model shall be modified in order to properly solve the whole dynamics of evaporation.

As a comparison, note that Eggers *et al.* [16] numerically studied the evaporation of a sessile droplet by coupling the hydrodynamics of the droplet with a self-consistent description of evaporation from the drop and the precursor film in a similar approach as Doumenc *et al.* [17]. They recovered the scaling of the late time radius $R \sim (t_0 - t)^\alpha$ with $\alpha \simeq 1/2$. However, no wetting law for

apparent contact angle was proposed. In some cases, dominant drying from the middle of the drop is even found at late times, the drops loses its spherical shape and is depleted at the center. This phenomenon is reminiscent of the negative values of apparent contact angle found in our model.

4 Conclusion

In this paper, we have described a model for completely wetting liquid under diffusive evaporation taking into account the divergent nature of the evaporative flux. A wetting law relating the apparent contact angle to the speed of the contact line was proposed and tentatively used to numerically study the dynamics of an evaporating droplet in total wetting conditions. This model correctly describes the early stages of spreading and retraction of a droplet. However, at late times, the contact angle vanishes before the radius vanishes itself, yielding non-physical scalings. Usual dynamical scalings found in experiments can only be recovered by extrapolating a final reference time.

Acknowledgement: The authors acknowledge support from ANR (DEPSEC 05-BLAN-0056-01) and wish to thank G. Berteloot, A. Boudaoud, P. Colinet, A. Daerr, F. Doumenc, J. Eggers together with A. Rednikov for enlightening discussions.

References

[1] R. D. Deegan, O. Bakajin, T. F. Dupont, G. Huber, S. R. Nagel & T. A. Witten, Capillary flow as the cause of ring stains from dried liquid drops, *Nature* 1997, **389**, 827.

[2] C. Poulard, G. Guéna, A. M. Cazabat, A. Boudaoud & M. Ben Amar, Rescaling the dynamics of evaporating drops, *Langmuir* 2005, **21**, 8226–8233.

[3] P.-G. de Gennes, Wetting: statics and dynamics, *Rev. Mod. Phys.* 1985, **57**, 827.

[4] D. Bonn, J. Eggers, J. Indekeu, J. Meunier & E. Rolley, Wetting and spreading, *Rev. Mod. Phys.* 2009, **81**, 739.

[5] V. M. Starov, M. G. Velarde & C. J. Radke, *Wetting and Spreading Dynamics* (CRC Press, 2007).

[6] M. G. Velarde, editor, *Eur. Phys. J. Special Topics*, vol. 197, 2011.

[7] G. Berteloot, C.-T. Pham, A. Daerr, F. Lequeux & L. Limat, Evaporation induced flow a near contact line: consequences on coating and contact angle, *Europhys. Lett.* 2008, **83**, 14003.

[8] D. Qu, E. Ramé & S. Garoff, Dip-coated films of volatile liquids, *Phys. Fluids* 2002, **14**, 1154.

[9] R. D. Deegan, O. Bakajin, T. F. Dupont, G. Huber, S. R. Nagel & T. A. Witten, Contact line deposits in an evaporating drop, *Phys. Rev. E* Jul 2000, **62** (1), 756–765.

[10] V. S. Ajaev, Spreading of thin volatile liquid dorplets on uniformly heated surfaces, *J. Fluid Mech.* 2005, **528**, 279.

[11] S. S. Panchamgam, S. J. Gokhale, J. L. Plawsky, S. DasGupta & P. C. Wayner Jr, Experimental determination of the effect of disjoining pressure on shear in the contact line region of a moving evaporating thin film, *J. Heat. Transfer* 2005, **127**, 231.

[12] Y. Pomeau, Contact line moving on a solid, *Eur. Phys. J. Special Topics* 2011, **197**, 15.

[13] A. Y. Rednikov & P. Colinet, Vapor-liquid steady meniscus at a superheated wall: Asymptotics in an intermediate zone near the contact line, *Microgravity Sci. Technol.* 2010, **22**, 249.

[14] S. Semenov, V. M. Starov, R. G. Rubio, H. Agogob & M. G. Velarde, Evaporation of sessile water droplets: Universal behaviour in presence of contact angle hysteresis, *Colloids and Surfaces A: Physicochem. Eng. Aspects* 2011, **391**, 135.

[15] C.-T. Pham, G. Berteloot, F. Lequeux & L. Limat, Dynamics of complete wetting liquid under evaporation, *Europhys. Lett.* 2010, **92**, 54005.

[16] J. Eggers & L. M. Pismen, Non local description of evaporating drops, *Phys. Fluids* 2010, **22**, 112101.

[17] F. Doumenc & B. Guerrier, A model coupling the liquid and gas phases for a totally wetting evaporative meniscus, *Eur. Phys. J. Special Topics* 2011, **197**, 281.

[18] N. Shahidzadeh-Bonn, S. C. Rafai, A. Azouni & D. Bonn, Evaporating droplets, *J. Fluid Mech.* 2006, **549**, 307.

[19] O. V. Voinov, Hydrodynamics of wetting, *Fluid. Dyn.* 1976, **11**, 714.

[20] H. P. Kavehpour, B. Ovryn & G. H. McKinley, Microscopic and macroscopic structure ofthe precursor layer in spreading viscous drops, *Phys. Rev. Lett.* 2003, **91**, 196104.

[21] C.-T. Pham, G. Berteloot, F. Lequeux & L. Limat, Dynamics of complete wetting liquid under evaporation (Erratum), *Europhys. Lett.* 2011, **93**, 69901.